This is the peer reviewed version of the following article: Monteiro, Hugo L.S.; Trindade, Marcelo A.. Performance analysis of proportional-integral feedback control for the reduction of stick-slip-induced torsional vibrations in oil well drillstrings. Journal of Sound and Vibration, 398:28-38, 2017, which has been published in final form at https://doi.org/10.1016/j.jsv.2017.03.013.

This article may be used for non-commercial purposes in accordance with Elsevier Terms and Conditions for Use of Self-Archived Versions. © 2021. This manuscript version is made available under the CC-BY-NC-ND 4.0 license https://creativecommons.org/licenses/by-nc-nd/4.0/.

# Performance analysis of proportional-integral feedback control for the reduction of stick-slip-induced torsional vibrations in oil well drillstrings

Hugo L.S. Monteiro<sup>a</sup>, Marcelo A. Trindade<sup>a,\*</sup>

<sup>a</sup> Department of Mechanical Engineering, São Carlos School of Engineering, University of São Paulo, 13566-590 São Carlos, Brazil.

### Abstract

The stick-slip phenomenon, in the process of drilling oil wells, can lead to large fluctuations in drill-bit angular velocity, due to the interaction between drill-bit and rock formation, and, thus, cause irreparable damage to the process. In this work, the performance of control laws applied to the rotary table (responsible for moving the drillstring) is analyzed, in order to reduce stick-slip and drill-bit angular velocity oscillations. The control laws implemented are based on a PI (Proportional-Integral) controller, for which the torque applied to the rotating table has components proportional and integral to the table angular velocity with constant or variable WOB (Weight-On-Bit). For the drillstring, a finite element model with a linear interpolation for the torsional motion was proposed. The torque at drill-bit was modeled considering a non-regularized dry friction model, with parameters that were adjusted using empirical data proposed in literature. Several performance criteria were analyzed and it was observed that a minimization of the mean deviation of the drill-bit angular velocity relative to the target one would provide the best operating condition. Parametric analyses of proportional and integral control gains were performed, yielding level curves for the mean deviation of drillbit angular velocity. From these curves, stability regions were defined in which the deviation is acceptable. These regions were observed to be wider for smaller values of WOB and higher values of target angular velocity and vice-versa. In addition, the inclusion of a controlled dynamic WOB was proposed leading to reduced levels of mean deviation of angular velocity and, thus, improving stability regions for the drilling process.

Keywords: Oil well drilling, torsional vibration control, stick-slip, drillstring dynamics

### 1. INTRODUCTION

The process of drilling oil wells, for oil or gas production, consists in opening a borehole in the rock formation by means of a rotating drill-bit whose rotation is driven by a torque drive system at the surface (top position) and a drillstring responsible for transmitting the torque from the drive system to the drill-bit (bottom position). Oil wells can reach up to 5 km deep with diameters between 10 and 85 cm. Therefore, the drillstring is mainly composed of a very slender structure, so-called drill-pipes, with external diameter of less than 15 cm and wall thickness of less than 10 mm. Only a relatively small lowest part of the drillstring (called drill-collars) is built using thick-walled tubes to avoid buckling [1, 2]. The drill-bit is part of a heavy

Email addresses: hugo.monteiro@yahoo.com.br (Hugo L.S. Monteiro), trindade@sc.usp.br (Marcelo A. Trindade)

<sup>\*</sup>Corresponding author.

component called BHA (Bottom-Hole Assembly) and is subjected to the driving torque applied through the drillstring, on one hand, and to a reaction torque from the bit-rock interaction, on the other hand [2, 3].

Due to the low torsional stiffness of the drillstring and the concurrent torques applied at drillstring top and bottom extremities, the drillstring may be subjected to high levels of torsional vibrations [4]. Depending on the operational conditions, the drillstring may also undergo lateral (bending) and axial (longitudinal) vibrations [1]. Drillstring vibration is one of the most important causes of malfunctioning, failure or inefficiency in the oil well drilling process [4, 5, 6]. In particular for the torsional vibrations, the drillstring may be twisted several turns leading to possible failure in the drill-pipes sections and connections. Also, when untwisting, the drillstring induces angular velocities much higher than the target ones at the drill-bit, which may lead to a mechanical failure of the drill-bit. In extreme cases, the angular velocity oscillation due to drillstring torsional vibration may lead to a complete standstill of the drill-bit (stick phase) whereas the drillstring is torqued-up until the drill-bit starts rotating again (slip phase). This phenomenon has been identified during several field observations [7] as periodic, stable, self-excited and low-frequency oscillations of drilling angular velocity which generally disappear as the target angular velocity is increased, although this tends to induce the augmentation of lateral vibrations.

Although the propagation of torsional waves along the drillstring may be determined by linear dynamic equations, the interaction between drill-bit and rock formation leads to a highly non-linear behavior [8, 9]. Richard and Detournay [10] studied the self-excited response of such systems using a discrete model with two degrees of freedom and they have shown that the coupling between torsional and normal modes in the drill-bit are sufficient to generate the stick-slip phenomenon. Other authors have also studied this phenomenon using discrete (lumped) structural models, for instance in [11, 12]. Continuous-based structural models have also been considered in the literature, as in [9, 13, 14, 15].

In terms of modeling of the interaction between drill-bit and rock formation, several models were proposed in the literature. The most popular for drillstring dynamics analyses are the phenomenological ones starting from a selected dry-friction model followed by curve-fitting of experimentally observed torque-angular velocity curves to adjust the parameters of the model [9, 14, 15]. These models can be divided in two groups: the ones in which the discontinuity in the torque-angular velocity curve for very low (and null) angular velocity (stick phase) is regularized and the ones in which the discontinuity is kept. In the former, the regularization allows to evaluate the torque between drill-bit and rock formation in terms of the angular velocity only using a continuous function. Several such functions were proposed and used in the literature [11, 13, 14, 15]. On the other hand, for non-regularized models, one has to deal with the torque-angular velocity curve discontinuity and, also, another criteria must be used to evaluate the torque in stick phase. Some previous works considered non-regularized models, such as [2, 12, 16].

Since stick-slip induced torsional vibrations have a central role in the drilling process, several different techniques have been proposed along the last two decades to automatically control this phenomenon or, at least, minimize its consequences. They can be summarized as: active damping [2], torsional rectification [17, 18], soft-torque [9, 17], proportional-integral (PI) angular velocity control [11, 12, 14] and PI control combined to dynamic weight-on-bit (WOB) variation [16, 19]. The main advantage of PI control is that it is already implemented in real drilling processes. More complex control techniques could be harder to implement since well established processes and equipments could have to be modified and they might also be more sensitive to system variabilities that are common in drilling processes.

In the present work, a finite element model for the drilling system combined to a non-regularized drill bit-rock formation interaction model is considered to evaluate the performance of two different control techniques, namely PI control and PI control combined to dynamic WOB, in terms of their control parameters. A methodology to establish and analyze so-called stability regions, for which the control is able to effectively minimize stick-slip, is proposed. The main contribution of the present work is to propose a methodology for establishing well performing ranges for PI control gains and, then, to show that a properly designed dynamic WOB may improve these ranges.

### 2. DRILLING SYSTEM DESCRIPTION AND MODELING

The drilling system, schematically represented in Figure 1, consists mainly of two rotary inertias, one at the top surface, so-called rotary or driving table, and one at the bottom end, so-called bottom-hole-assembly (BHA). The driving table has a large rotary inertia  $J_t$  to prevent sudden changes in drilling angular velocity and is subjected to an applied driving torque  $T_t$ . The BHA is composed of the drill-bit (rock cutting/crushing device), heavy and bending stiff drill-collars, and stabilizers to prevent transversal motion and thus change in drilling direction. The BHA is considered to behave as a rigid body with rotary inertia  $J_b$  and is subject to a reaction torque  $T_b$  applied by the rock formation during the drilling (rock cutting/crushing) process. These two rotary inertias are interconnected through a very long and flexible link, so-called drillstring, composed by a series of end-to-end screwed drill-pipes. The drill-pipes are made of uniform and homogeneous metallic tubes with inner and outer radius,  $R_i$  and  $R_o$ , and the following material properties: mass density  $\rho$  and shear modulus G. Drilling system geometrical and material properties are summarized in Table 1.

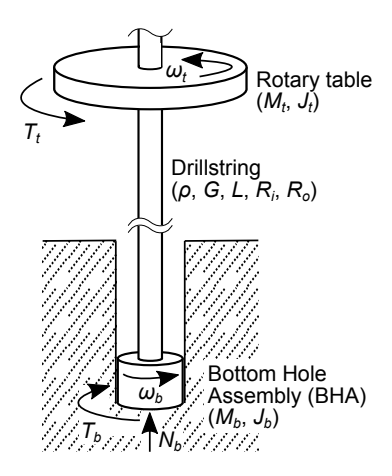


Figure 1: Schematic representation of considered drilling system.

A discrete model for the drillstring is constructed using unidimensional finite elements with Lagrange linear interpolation functions, leading to two nodes and two torsional rotation angles degrees-of-freedom per element. For more details on the two-node torsional finite element, see [20]. In all cases studied in this work, 10 finite elements for the drillstring were proven to be accurate enough. Linear elastic material behavior and infinitesimal strains are considered for the drillstring. The drilling system is also subjected to an equivalent viscous damping, proportional to the stiffness matrix  $\mathbf{D} = \alpha \mathbf{K}$ , with  $\alpha = 0.01$ , due to the drilling mud surrounding it and other types of energy dissipation such as friction forces between stabilizers

Table 1: Geometrical and material parameters considered for the drilling system [9].

Property	Value
Drillstring mass density, $\rho$ (kg m <sup>-3</sup> )	8010
Drillstring shear modulus, $G$ (GPa)	79.6
Drillstring length, $L$ (m)	3000
Outer radius of drillstring, $R_o$ (m)	0.0635
Inner radius of drillstring, $R_i$ (m)	0.0543
Driving table rotary inertia, $J_t$ (kg m <sup>2</sup> )	500
BHA rotary inertia, $J_b$ (kg m <sup>2</sup> )	394

and drilled well walls. This leads to equivalent linear damping factors that are both reasonable for practical drilling conditions and also that increase in frequency as expected for the different damping sources present in drilling process. Using these assumptions, a set of discrete linear equations of motion, that represent the drilling system dynamics, can be written as

$$\mathbf{M}\ddot{\mathbf{u}} + \mathbf{D}\dot{\mathbf{u}} + \mathbf{K}\mathbf{u} = \mathbf{F}_t + \mathbf{F}_b,\tag{1}$$

where  $\mathbf{M}$ ,  $\mathbf{D}$  and  $\mathbf{K}$  are the mass, damping and stiffness matrices.  $\mathbf{u}$  is the vector of nodal angular displacement, or torsional rotation angles, and  $\mathbf{F}_t$  and  $\mathbf{F}_b$  are the vector of nodal applied torques, at top driving table and at bottom end due to bit-rock interaction, respectively.

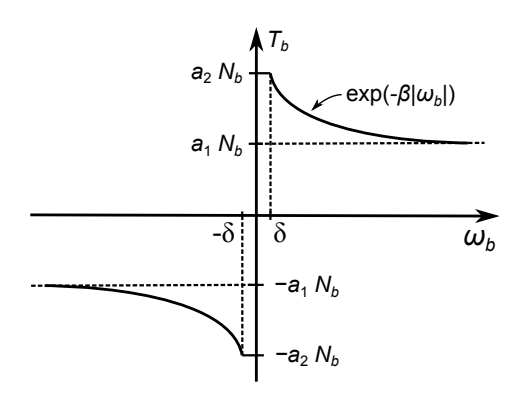


Figure 2: Representation of dry friction model considered for the drill bit-rock formation interaction.

The reaction torque due to the interaction between drill bit and rock formation is modeled using a non-regularized dry friction model similar to the one used in [12, 16]. In this model, the reaction torque is described using a function (2) that can be divided in three situations: 1) During the stick phase, that is when the drill-bit angular velocity modulus is equal to or smaller than a threshold value  $\delta$ , the reaction torque is equal (opposite in sign) to the torque applied to the drill-bit by the drillstring provided it does exceed the maximum allowable reaction torque  $|T_b^{max}| = a_2 N_b$ ; 2) During the slip phase, that is when the drill-bit angular velocity modulus is larger than  $\delta$ , the reaction torque modulus decays exponentially from the maximum allowable torque  $a_2 N_b$  down to a limiting torque value  $a_1 N_b$  corresponding to higher angular

velocities.

$$T_{b} = T, for |\omega_{b}| \leq \delta \text{ and } |T| \leq a_{2}N_{b},$$

$$T_{b} = a_{2}N_{b}sgn(T), for |\omega_{b}| \leq \delta \text{ and } |T| > a_{2}N_{b},$$

$$T_{b} = [a_{1} + (a_{2} - a_{1})e^{-\beta|\omega_{b}|}]N_{b}sgn(\omega_{b}), for |\omega_{b}| > \delta.$$

$$(2)$$

The threshold value  $\delta$  for the angular velocity that controls the transition between stick and slip phases is considered to be  $\delta = 0.0001$  rad/s in this work. The torque applied to the drill-bit by the drillstring, T, which is only used during the stick phase, is approximated by the product between the equivalent torsional stiffness of the drillstring finite element adjacent to the drill-bit,  $GJ/L_e$ , and the difference between the angular displacements at these element nodes. The normal force  $N_b$  is equal to the weight-on-bit (WOB) set for the drilling operation.  $L_e$  is the length of the finite element adjacent to the drill-bit and J is the polar moment of area of the drillstring cross-section,  $J = (\pi/2)(R_o^4 - R_i^4)$ , where  $R_o$  and  $R_i$  are the outer and inner radii of the drillstring, respectively.

The dry friction model parameters  $a_1$ ,  $a_2$  and  $\beta$  were identified to approximate the phenomenological model for the reaction torque in terms of the drill-bit angular velocity proposed by Tucker and Wang [9] based on drilling measurements under stable drilling conditions. Table 2 presents the identified dry friction model parameters for five values of WOB:  $\{80, 100, 120, 140, 160\}$  kN. The reaction torques at drill-bit as function of drill-bit angular velocity predicted by the dry friction model for the different WOB are presented in Figure 3.

Table 2: Dry friction model pameters  $a_1$ ,  $a_2$  and  $\beta$  for five values of WOB based on [9].

WOB $(kN)$	80	100	120	140	160
$a_1 \text{ (m)}$	0.037	0.032	0.029	0.026	0.025
$a_2 \text{ (m)}$	0.057	0.070	0.079	0.085	0.089
$\beta$ (s rad <sup>-1</sup> )	0.082	0.093	0.097	0.098	0.099

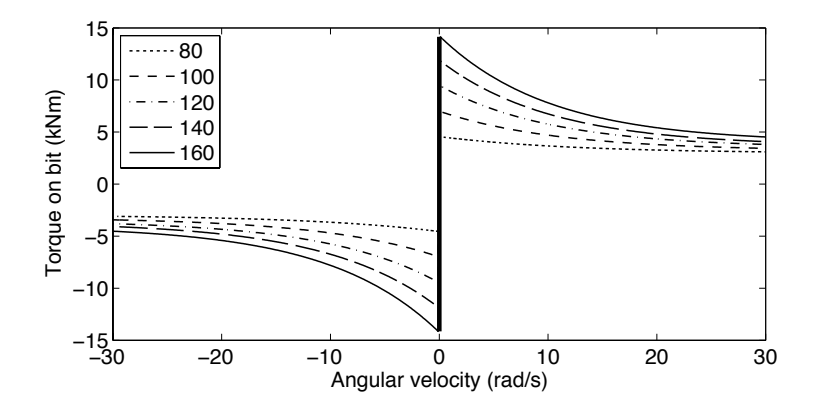


Figure 3: Torque on bit as function of drill-bit angular velocity predicted by the dry friction model for several WOB: 80 kN (dot), 100 kN (short dash), 120 kN (dash-dot), 140 kN (long dash), 160 kN (solid).

### 3. ANGULAR VELOCITY CONTROL DESIGN

The standard control technique used to set the target angular velocity of the drilling operation considers only the information available at the driving table (angular velocity), as depicted in Figure 4. The control torque  $T_t$  is responsible for driving the rotary motion of the drillstring and, consequently, the drill-bit. In general, a feedback control strategy is used to evaluate the control torque with the objective of maintaining a constant target angular velocity. The most commonly used is a proportional-integral (PI) controller such that

$$T_t = K_p(\omega_{ref} - \omega_t) + K_i(\omega_{ref}t - \theta_t). \tag{3}$$

The driving control torque  $T_t$  is thus only dependent on how the angular velocity  $\omega_t$  and displacement  $\theta_t$  at the driving table deviates from the reference (desired or target) corresponding values,  $\omega_{ref}$  and  $\omega_{ref}t$ . However, due to the drillstring high flexibility and, thus, expected torsional vibrations, on one hand, and the high frictional reaction torque at the drill-bit, on the other hand, this control technique does not guarantee a constant target angular velocity  $\omega_b$  at the drill-bit. Indeed, experimental observations indicate that this control strategy will normally lead to a fluctuating drill-bit angular velocity.

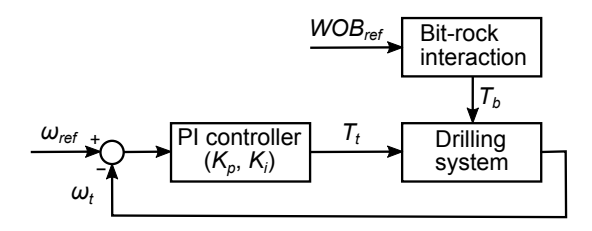


Figure 4: Proportional-integral (PI) angular velocity control scheme.

It is well-known that these stick-slip oscillations tend to diminish by either increasing the target angular velocity or reducing the weight-on-bit [1]. The former, however, may also lead to transversal vibrations which may yield other drilling failure modes and, thus, is normally avoided. The reduction of the weight-on-bit, whenever stick-slip oscillations are observed, is therefore the strategy generally considered in field operation. This can be done by increasing the hook-load at the top assembly. However, a reduction in the target weight-on-bit diminishes directly the drilling performance in terms of rate of penetration, which is approximately linearly proportional to weight-on-bit and drill-bit angular velocity [9].

On the other hand, based on this frequently-used manual technique of reducing the weight-on-bit whenever angular velocity oscillations are observed, it is possible to consider an automatic (dynamic) weight-on-bit variation in terms of the angular velocity. This idea has been studied in [16] in which the WOB is decomposed in two terms, one being the target WOB and another one that is proportional to the modulus of the drill-bit angular velocity. Thus, whenever drill-bit angular velocity increases, the actual weight-on-bit is also increased. Their results indicate that the stick-slip phenomenon is reduced. However, the drill-bit angular velocity is generally not known or measurable.

Based on previous observations that angular velocity oscillations at rotary table and at drill-bit are in phase [12, 14], it is proposed that the dynamic WOB variation could be written in terms of the angular

velocity at the rotary table, and not at the drill-bit, such that

$$WOB = WOB_{ref} + K_w(\omega_t - \omega_{ref}), \text{ with } K_w \ge 0.$$
 (4)

Therefore, if the angular velocity  $\omega_t$  is larger than the reference one, the weight-on-bit is increased relative to the target one (which allows higher rate of penetration). But, in the opposite case, where the angular velocity  $\omega_t$  is smaller than the target one, meaning that stick-slip is potentially occurring, the weight-on-bit is reduced to alleviate the frictional reaction torque. If target and actual angular velocities are equal, the actual weight-on-bit is equal to the target one. In all cases, the control torque remains based on the previously presented PI controller (3), as schematically represented in Figure 5.

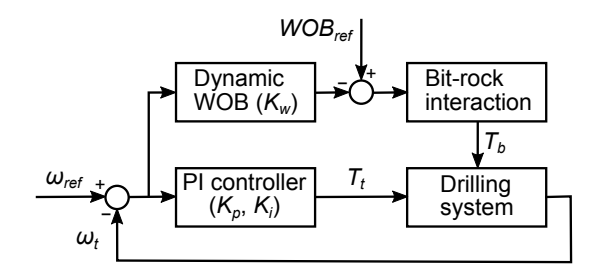


Figure 5: PI angular velocity control scheme with dynamic weight-on-bit (WOB).

It is clear that the WOB variation control gain  $K_w$  is limited according to the maximum allowable variations in the hook-load that would be used in practice to vary the weight-on-bit dynamically. Thus, the control gain  $K_w$  is limited so that the actual weight-on-bit variations are smaller than 15%-20% of the target weight-on-bit.

### 4. RESULTS AND DISCUSSIONS

Considering the drilling system described previously, this section presents some results obtained for the PI controlled drilling aiming at, first, verifying the proposed finite element model and, then, performing a parametric analysis to determine optimal values and satisfactory regions of the PI control gains. Finally, an additional controller with the objective of varying the WOB is proposed, designed and evaluated.

# 4.1. Verification of FE model combined to a non-regularized friction model for the actively controlled drilling system

As a first analysis, the drilling condition previously studied in [9, 14], in which the stick-slip phenomenon is clearly observed, is considered. The weight-on-bit is constant and equal to 120 kN and the target (reference) angular velocity is 100 rpm (10.47 rad/s). The PI control gains are set to  $K_p = 200$  Nms and  $K_i = 100$  Nm. For the simulation, it is considered that the entire drilling system (drive table, drillstring and BHA) is rotating freely at 70 rpm and, then at time t = 0 s, the drill-bit touches the rock formation. The time response of the system is simulated in the time interval t = [0, 100]s using MATLAB(R) ODE integrator ode45. The same simulation was performed in [9, 14] but, in both cases, a regularized dry friction model was considered for the evaluation of the torque-on-bit (reaction torque due to interaction between drill-bit

and rock formation). Notice that the discontinuous friction model, considered in the present work, leads to an added computational effort since the numerical integration algorithm is required to reduce the step size significantly whenever the system is in or near the stick phase. The algorithm adapts the step size so that a maximum error tolerance is respected. In the present work, a relative error tolerance of  $10^{-3}$  was considered.

Figure 6 shows the time response of angular velocities and torques at drill-bit and rotary table for the drilling condition studied in [9, 14]. The overall behavior and dynamic properties, such as angular velocity oscillations frequency and amplitudes, torque amplitudes, relative amplitudes between velocities and torques at drill-bit and rotary table, are very similar to those presented in [9, 14], except for the stick phase that is only captured in the present study.

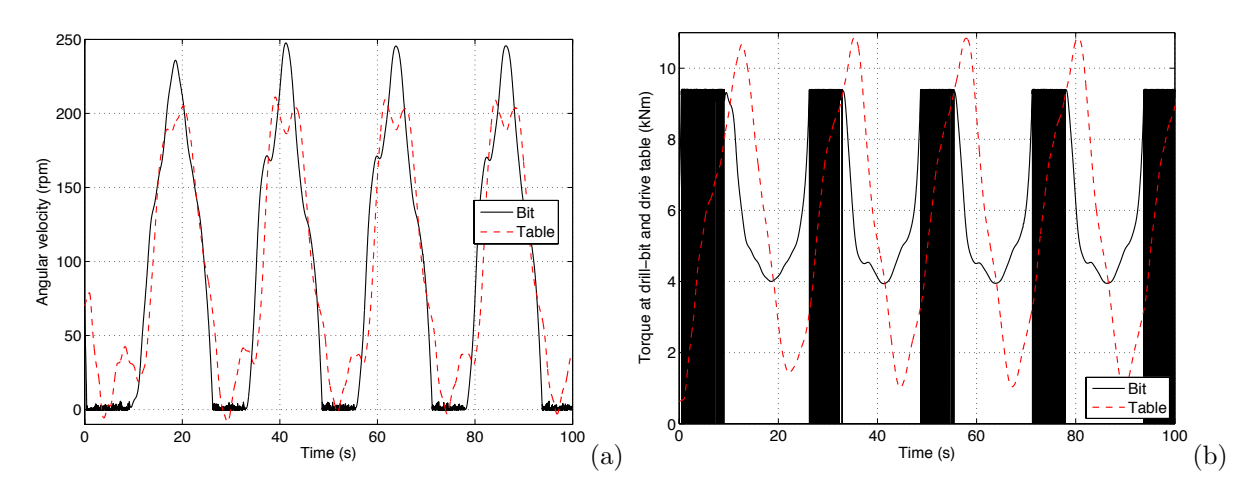


Figure 6: Time response of angular velocities (a) and torques (b) at drill-bit and drive table for the drilling condition studied in [9, 14].

It is noticeable that for the considered drilling condition and control gains, the stick-slip phenomenon is well sustained and the angular velocity at the drill-bit can reach up to more than double of the target angular velocity. This is clearly an undesired behavior and one should search for mitigation solutions other than increasing target angular velocity and reducing weight-on-bit.

## 4.2. Parametric analysis of PI control gains for drilling control performance

In this section, a parametric analysis is performed by varying the proportional and integral control gains,  $K_p$  and  $K_i$ , in order to search for better time response behaviors with potential mitigation of stick-slip phenomenon and its consequences. For that, an overall performance criteria is defined in terms of the average deviation from the drill-bit target angular velocity, written as

$$J = \frac{1}{\Delta t} \int_{\tau}^{\tau + \Delta t} \frac{|\omega_b - \omega_{ref}|}{\omega_{ref}} dt.$$
 (5)

This metric combines deviation amplitude and settling time and is to be minimized by proper choice of PI control gains. Then, a regular grid of control gains pairs is defined and the average angular velocity deviation J is evaluated for each control gains pair. In the present case, the following time values were

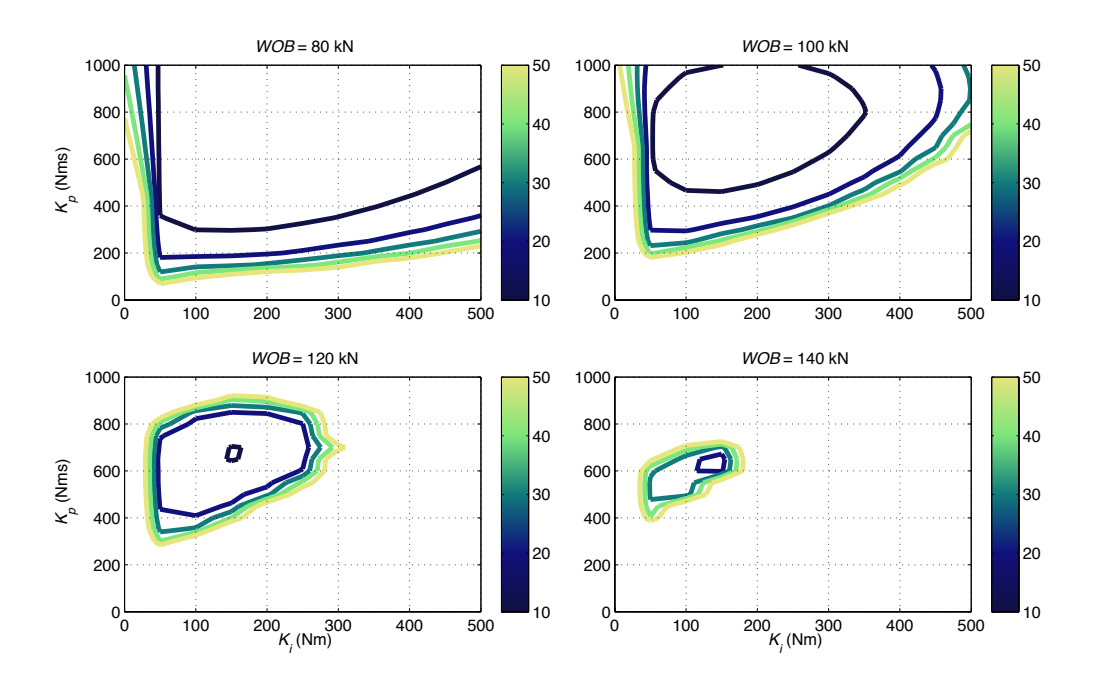


Figure 7: Contour plots of angular velocity average deviation J (in percent) in terms of control gains  $K_p$  and  $K_i$  for several target WOB and target angular velocity of 100 rpm.

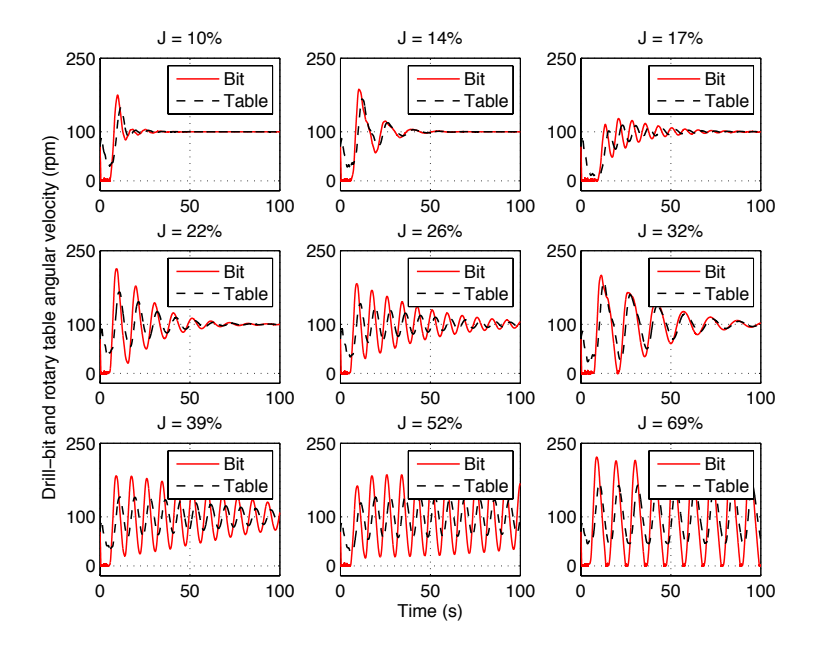


Figure 8: Time responses for different control gain pairs (angular velocity average deviation, J, in percent) with target WOB of 120 kN and target angular velocity of 100 rpm.

considered to evaluate the integral:  $\tau = 0$  and  $\Delta t = 100$  s. Figure 7 shows contour plots of the average angular velocity deviation J (in percent) considering several PI control gains pairs, for target angular velocity of 100 rpm and for target WOB of 80, 100, 120 and 140 kN. The contour lines correspond to the values of

 $J = \{10, 20, 30, 40, 50\}\%$ . It is noticeable that for lower values of WOB (80 and 100 kN), it not difficult to find a PI control gains pair that leads to an average angular velocity deviation below 10%. However, as the WOB value is increased, it becomes harder and harder to do so. For a WOB of 120 kN, only a very small region of control gains pairs allow such performance (around  $K_p = 675$  Nms and  $K_i = 150$  Nm) while, for a WOB of 140 kN, such performance is not possible. To illustrate how a given average angular velocity deviation index relates to the angular velocity time response, Figure 8 presents the time responses for different control gains pairs, leading to different deviation indexes, considering a target WOB of 120 kN and a target angular velocity of 100 rpm. Notice that for larger values of deviation (larger than 50% for instance), the angular velocity oscillations are clearly persistent and probably accompanied by several occurrences of drill-bit stick phases.

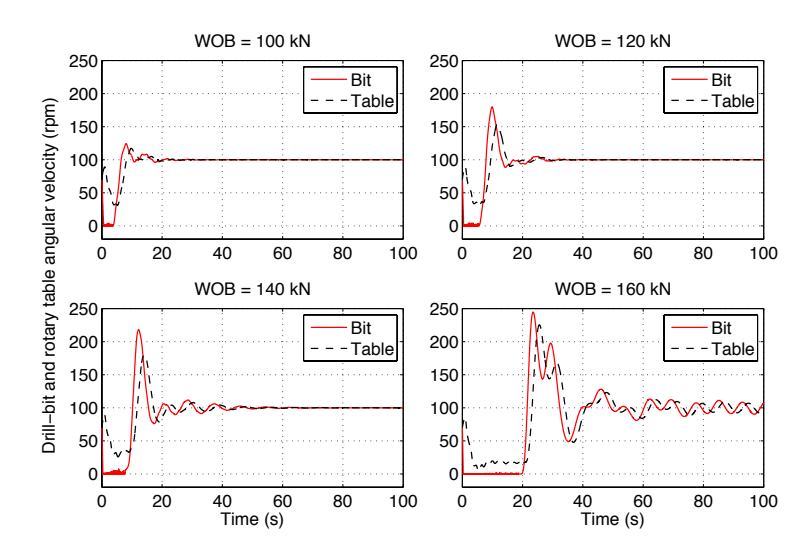


Figure 9: Time responses for optimal control gain pairs for target angular velocity of 100 rpm and target WOB of [100, 120, 140, 160] kN.

Optimal PI control gains for each drilling operating condition may also be found from this parametric analysis. Figure 9 shows the time responses for the optimal PI control gains considering a target angular velocity of 100 rpm and four values of target WOB:  $\{100, 120, 140, 160\}$  kN. It can be observed in Figure 9 that, for WOB values of 100 kN and 120 kN, the angular velocity converges very fast to the target value while the overshoot is kept smaller than 100%. In terms of the average angular velocity deviation index, both cases yield index values smaller than 10% (5.8% for 100 kN and 9.9% for 120 kN). On the other hand, for higher WOB values (140 and 160 kN), both settling time and overshoot become more important leading to higher deviation index values (15% for 140 kN and 35% for 160 kN). In the case of WOB value of 160 kN, a fine tuning of control gains was necessary since the region of lower deviation indexes is not large. Table 3 shows the optimal PI control gains,  $K_p$  and  $K_i$ , and average angular velocity deviation indexes, J, for different target WOB.

### 4.3. Design and evaluation of controlled WOB variation for drilling performance improvement

It is clear from the previous section that by increasing the target WOB, the optimal drilling performance (in terms of average angular velocity deviation) is worsened and the region of acceptable PI control gains

Table 3: Optimal PI control gains,  $K_p$  and  $K_i$ , and average angular velocity deviation indexes, J, for different target WOB.

WOB (kN)	$K_p$ (Nms)	$K_i$ (Nm)	J~(%)
100	675	125	5.8
120	675	175	9.9
140	650	150	15.0
160	512	63	35.4

pairs is shrinked (so that it is harder and harder to find a control gains pair that leads to acceptable performance). It is then proposed to search for an improvement in both optimal performance and region of acceptable performance by considering a controlled dynamic weight-on-bit variation as previously presented. Therefore, a second parametric analysis was performed by varying the WOB variation control gain  $K_w$ , according to (4). To find both optimal control gains and regions of acceptable performance, for each WOB variation control gain  $K_w$ , the time responses and average angular velocity deviations were evaluated for the previously considered PI control gains pairs  $(K_p$  and  $K_i)$ .

A preliminary analysis of the effect of dynamic WOB control gain  $K_w$  has shown that: i) each PI control gains pair may lead to a different optimal dynamic WOB control gain, but it is almost always possible to decrease the average angular velocity deviation; ii) dynamic WOB control gain may enlarge the region of acceptable performance significantly, but by using different WOB control gains for different PI control gains pairs; iii) dynamic WOB control gain should be limited so that the actual weight-on-bit variations are smaller than 15%-20% of the target weight-on-bit. Based on these general remarks, it was chosen to select a single dynamic WOB control gain  $K_w$  for each drilling condition, limited to  $\{1, 1.2, 1.4, 1.7 \text{ and } 2\}$  kNs for the target WOB of  $\{80, 100, 120, 140 \text{ and } 160\}$  kN, respectively. Under these restrictions,  $K_w$  was selected so that the region of acceptable performance is enlarged and the minimum average angular velocity deviation is not increased.

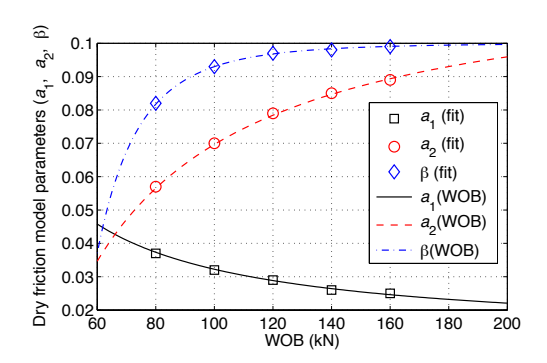


Figure 10: Interpolation of dry friction model parameters for intermediate values of WOB.

In order to consider a varying WOB, the dry friction model parameters, that were fitted to previous results and are presented in Table 2, need to be interpolated to account for intermediate values of WOB. This was done here through a curve-fitting procedure, such that a reasonable curve-fit is guaranteed for WOB values between 60 and 200 kN. The following expressions are obtained for the friction model parameters  $a_1$ 

(in meters),  $a_2$  (in meters) and  $\beta$  as functions of the WOB (in kN),

$$a_1(WOB) = 0.0119 + \frac{2.034}{WOB}; \ a_2(WOB) = 0.1222 - \frac{5.254}{WOB}; \ \beta(WOB) = 0.1 - 0.007(WOB/100)^{-4.3}.$$
 (6)

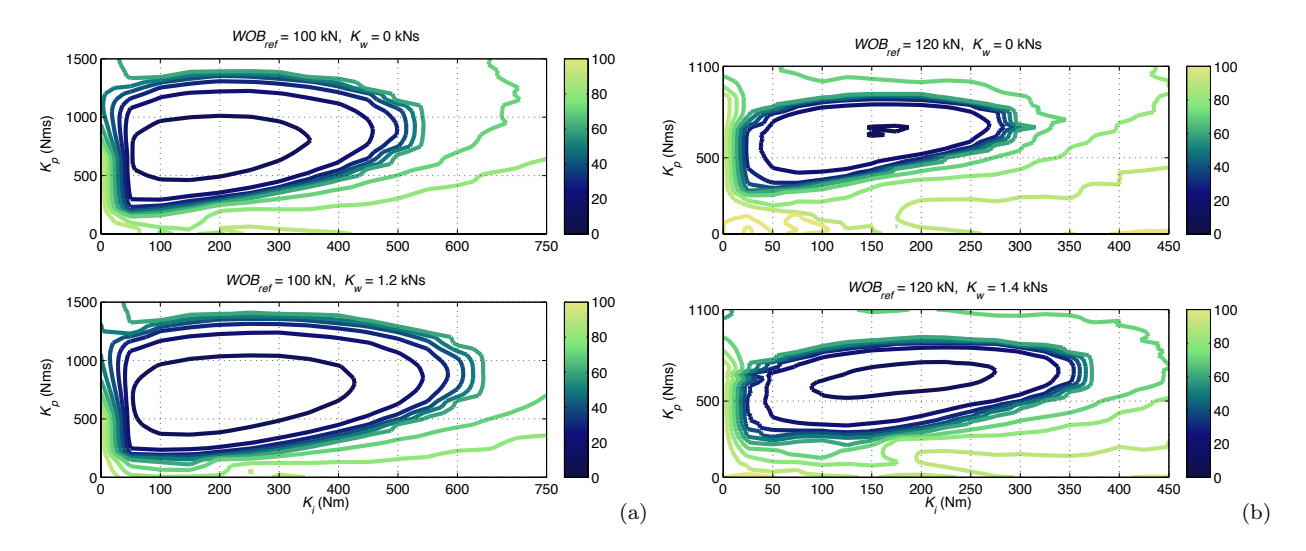


Figure 11: Contour plots of angular velocity average deviation J (in percent) in terms of control gains  $K_p$  and  $K_i$  for  $\omega_{ref} = 100$  rpm with constant (uncontrolled) and dynamic (controlled) WOB: (a)  $WOB_{ref} = 100$  kN; (b)  $WOB_{ref} = 120$  kN.

Figure 11 shows the contour plots of angular velocity average deviation J (in percent) in terms of control gains  $K_p$  and  $K_i$  for  $\omega_{ref} = 100$  rpm with constant (uncontrolled) and dynamic (controlled) WOB when the target WOB is set to 100 kN (Figure 11a) and 120 kN (Figure 11b). In both cases, it is possible to note that the region with deviation indexes below 10% is well enlarged, specially for WOB of 120 kN where the number of PI control gains choices seems to be largely increased when combined to a dynamic WOB variation control. Notice that the regions for other deviation levels are enlarged as well.

The same analysis can be done for higher target WOB of 140 and 160 kN. The corresponding contour plots are shown in Figures 12a and 12b, respectively. Unlike the previous ones, in these cases, the optimal PI control gains and the regions of acceptable performance are modified by the WOB control. For a WOB of 140 kN, the optimal PI control gains are modified from  $K_p = 650$  Nms and  $K_i = 150$  Nm (for constant WOB) to  $K_p = 600$  Nms and  $K_i = 200$  Nm. The region delimiting the 20% level for the average angular velocity deviation is significantly enlarged (and displaced to the right). Others contour lines, but not all, are enlarged as well. For the higher WOB of 160 kN, the contour plot is substantially modified when a dynamic WOB control is considered (Figure 12b). All regions are enlarged and some levels that were not visible before for constant WOB are now visible. The optimal PI control gains are modified from  $K_p = 512$  Nms and  $K_i = 63$  Nm (for constant WOB) to  $K_p = 550$  Nms and  $K_i = 175$  Nm.

Previous results indicate that the dynamic WOB variation should be considered in order to enlarge the regions of acceptable performance. However, it does not seem to affect too much the performance when optimal PI control gains are used. Figure 13 shows the time response of drill-bit angular velocity, control torque at drive table and dynamic WOB variation for a target WOB of 120 kN and optimal PI control gains. It can be observed that the dynamic WOB does allow a reduction of the maximum drill-bit angular

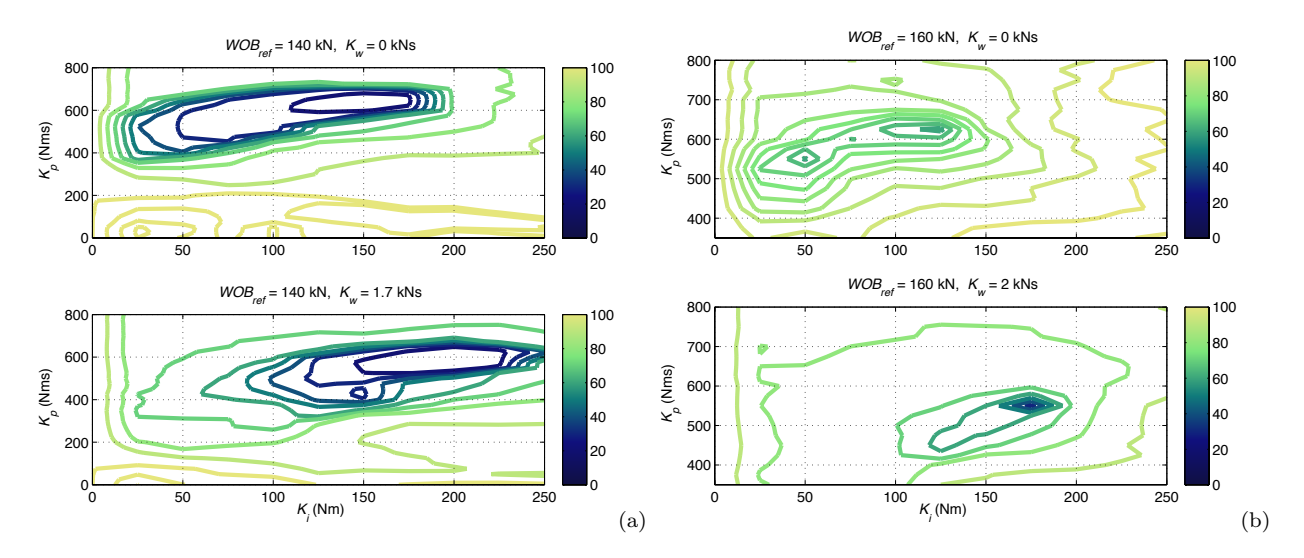


Figure 12: Contour plots of angular velocity average deviation J (in percent) in terms of control gains  $K_p$  and  $K_i$  for  $\omega_{ref}=100$  rpm with constant (uncontrolled) and dynamic (controlled) WOB: (a)  $WOB_{ref}=140$  kN; (b)  $WOB_{ref}=160$  kN.

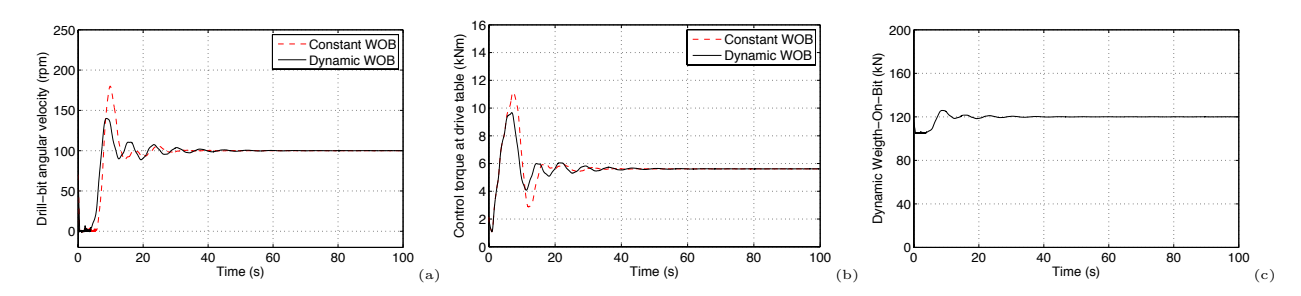


Figure 13: Time responses of drill-bit angular velocity (a), PI control torque (b) and dynamic WOB variation (c) for target WOB of 120 kN.

velocity but with similar settling time, compared to the case with constant WOB, leading to a reduction of 18% (from 9.9 to 8.2%) in the average angular velocity deviation (Figure 13a). In addition, the dynamic WOB variation also leads to a reduction of 12% in the PI control torque (from 11 to 9.6 kNm, Figure 13b). The dynamic WOB is presented in Figure 13c. The analysis for the WOB of 100 kN is not shown here since the improvement in the time response is negligible, although the PI control torque is reduced in 8%.

For the higher WOB values of 140 and 160 kN, the dynamic WOB also yields a reduction in both average angular velocity deviation and PI control torque. For 140 kN WOB, the angular velocity overshoot is reduced and the initial stick phase is abbreviated (Figure 14a) leading to a reduction in the average angular velocity deviation of 11% (from 15 to 13.3%). The PI control torque is also somewhat reduced (in 9%, from 13.7 to 12.5 kNm) when using a dynamic WOB (Figure 14b). The dynamic WOB is shown in Figure 14c.

The initial stick phase is substantially abbreviated by the dynamic WOB in the case of 160 kN target WOB with optimal PI control gains. Thus, although the maximum angular velocity is not significantly changed, the average angular velocity deviation is reduced in 28% (from 35.8 to 25.6%) compared to the case of constant WOB (Figure 15a). The PI control torque, that is only reduced in 4% (from 15.3 to 14.6 kNm), and the dynamic WOB are shown in Figures 15b and 15c, respectively.

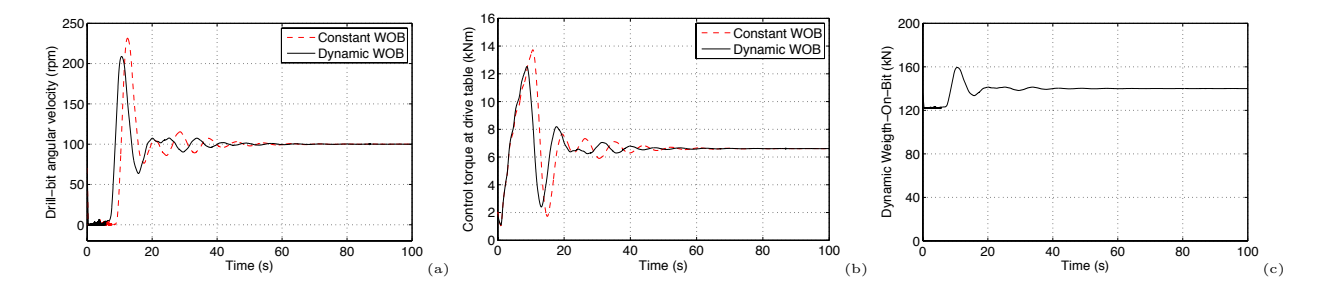


Figure 14: Time responses of drill-bit angular velocity (a), PI control torque (b) and dynamic WOB variation (c) for target WOB of 140 kN.

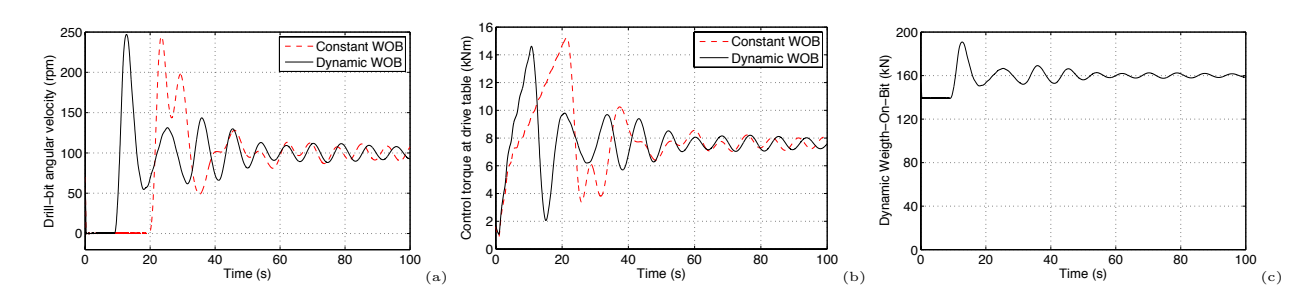


Figure 15: Time responses of drill-bit angular velocity (a), PI control torque (b) and dynamic WOB variation (c) for target WOB of 160 kN.

### 5. CONCLUSIONS AND FUTURE WORKS

A performance analysis of active control solutions for the reduction of stick-slip-induced torsional vibrations in oil well drillstrings was presented. A control law based on PI controller was implemented and applied to a parametric analyses of the proportional and integral control gains, yielding level curves for the average deviation of drill-bit angular velocity from which so-called stability regions, where the average deviation is acceptable, were defined. These regions were observed to be wider for smaller values of WOB and higher values of target angular velocity and vice-versa. In addition, the inclusion of a properly tuned controlled dynamic WOB was proposed leading to reduced levels of average angular velocity deviation and, thus, improving stability regions for the drilling process. Future works will be directed to other active control solutions that might improve drilling performance and to the evaluation of the effect of parametric uncertainties of the bit-rock interaction behavior on the drilling performance.

### ACKNOWLEDGEMENTS

The authors acknowledge the support of MCT/CNPq/FAPEMIG National Institute of Science and Technology on Smart Structures in Engineering, Grant 574001/2008-5, and the National Council for Scientific and Technological Development (CNPq), Grants 306675/2011-0 and 309193/2014-1.

### REFERENCES

[1] P. Spanos, A. Chevallier, N. Politis and M. Payne, Oil and gas well drilling: a vibrations perspective, *Shock and Vibration Digest* 35 (2) (2003) 85-103.

- [2] J.D. Jansen and L. van den Steen, Active damping of self-excited torsional vibration in oil well drillstrings, *Journal of Sound and Vibration* 179 (4) (1995) 647-668.
- [3] N. Mihajlovic, N. van de Wouw, M.P.M. Hendriks and H. Nijmeijer, Friction-induced limit cycling in flexible rotor systems: an experimental drill-string set-up, *Nonlinear Dynamics* 46 (3) (2006) 273-291.
- [4] J.F. Brett, The genesis of torsional drillstring vibrations, SPE Drilling Engineering 7 (3) (1992) 168-174.
- [5] Schlumberger Ltd., Shock and vibration in the drilling environment, Tutorial video, 8min20s, http://www.slb.com/services/drilling.aspx, 2006.
- [6] Y.A. Khulief and H. Al-Naser, Finite element dynamic analysis of drillstrings, Finite Elements in Analysis and Design 41 (2005) 1270-1288.
- [7] J.C.R. Placido, H.M.R. Santos and Y.D. Galeano, Drillstring vibration and wellbore instability, *Journal of Energy Resources Technology* 124 (2002) 217-222.
- [8] P.D. Spanos, A.K. Sengupta, R.A. Cunningham and P.R. Paslay, Modeling of roller cone bit lift-off dynamics in rotary drilling, *Journal of Energy Resources Technology* 117 (1995) 197-207.
- [9] R.W. Tucker and C. Wang, Torsional vibration control and cosserat dynamics of a drill-rig assembly, *Meccanica* 38 (2003) 143-159
- [10] T. Richard and E. Detournay, Stick-slip motion in a friction oscillator with normal and tangential mode coupling, *Comptes Rendus de l'Académie des Sciences Série IIb* 328 (2000) 671-678.
- [11] A.P. Christoforou and A.S. Yigit, Fully coupled vibrations of actively controlled drillstrings, *Journal of Sound and Vibration* 267 (2003) 1029-1045.
- [12] L.M. Manzatto and M.A. Trindade, Analysis of stability and performance of an oil well drilling operation subject to stick-slip using non-collocated linear velocity control, *Proceedings of 21st ABCM International Congress of Mechanical Engineering (COBEM)*, October 24-28, Natal, RN, Brazil, 2011.
- [13] R.W. Tucker and C. Wang, An integrated model for drill-string dynamics, Journal of Sound and Vibration 224 (1) (1999) 123-165.
- [14] M.A. Trindade and R. Sampaio, Active control of coupled axial and torsional drill-string vibrations, Proceedings of 18th ABCM International Congress on Mechanical Engineering (COBEM), Ouro Preto, MG, in CD-ROM, 2005.
- [15] T.G. Ritto, C. Soize and R. Sampaio, Non-linear dynamics of a drill-string with uncertain model of the bit-rock interaction, International Journal of Non-Linear Mechanics 44 (2009) 865-876.
- [16] E.M. Navarro-López and R. Suárez, Practical approach to modeling and controlling stick-slip oscillations in oilwell drill-string, Proceedings of the 2004 IEEE International Conference on Control Applications, Taipei, Taiwan, 1454-1460, 2004.
- [17] R.W. Tucker and C. Wang, On the effective control of torsional vibrations in drilling systems, Journal of Sound and Vibration 224 (1) (1999) 101-122.
- [18] E. Kreuzer and M. Steidl, Controlling torsional vibrations of drill strings via decomposition of traveling waves, *Archives of Applied Mechanics* (82) (2012) 515-531.
- [19] H. Puebla and J. Alvarez-Ramirez, Suppression of stick-slip in drillstrings: a control approach based on modeling error compensation, *Journal of Sound and Vibration* 310 (2008) 881-901.
- [20] S.S. Rao, Mechanical Vibrations, 5th edition, Pearson Prentice Hall, Upper Saddle River, NJ, 2011.